

# Vibration and Stability of an Axially Moving and Spinning Rayleigh Beam

Jer-Rong Chang\*, Wei-Jr Lin\*\*, Ying-Chung Chen\*\*\*, Siu-Tong Choi\*\*\*\* and Chun-Jung Huang\*\*\*\*\*

**Keywords** : axially moving, spinning, vibration, stability, Rayleigh beam.

## ABSTRACT

In this paper, Rayleigh beam theory and the finite element method with variable-domain element are used to derive the equations of motion of an axially moving and spinning beam with circular cross section. The rotary inertia and gyroscopic effect are taken into account. The dynamical behavior of the system is observed for cases of different types of axial motion. For stability analysis of a spinning beam with constant-speed axial extension deployment, eigenvalues of equations of motion are obtained to determine its stability, while Floquet theory is employed to investigate the stability of a spinning beam with periodical axial motion. Effect of the spinning speed of the beam on its vibration and stability is studied. Direct time numerical integration, based on a Runge-Kutta algorithm, is used to confirm the results from Floquet theory.

## INTRODUCTION

Dynamic behaviors of an axially moving or spinning beam have been studied extensively. Nevertheless, axially moving motion and spinning motion are usually seen in the operations of many mechanisms, and combined effects of these motions on stability of beam have not been considered. The equations of motion of the beam undergoing coupled motion of axially moving and spinning movements are derived. The stability of the beam is discussed in

*Paper Received June, 2020. Revised September, 2022. Accepted October, 2022. Author for Correspondence: Ying-Chung Chen.*

\* Associate Professor, Department of Aircraft Engineering, Air Force Institute of Technology, Kaoshiung, Taiwan 802, ROC.

\*\* Engineer, Department of Steel Research and Development, China Steel Corporation, Kaoshiung, Taiwan 812, ROC.

\*\*\* Associate Professor, Department of Aeronautical and Mechanical Engineering, Air Force Academy, Kaoshiung, Taiwan 802, ROC.

\*\*\*\* Professor, Department of Aeronautics and Astronautics, National Cheng Kung University, Tainan, Taiwan 701, ROC.

\*\*\*\*\* Assistant Professor, Institute of Aircraft and Maintenance, Far East University, Tainan, Taiwan 744, ROC.

this study.

An extensive review of the early literature in the domain of axially moving materials, such as traveling strings, tapes, cables, beams, and plates, was provided by Mote (1972). It includes the work that was done in the areas of band-saws, traveling string, power transmission belts, textile fiber, chain drives, pipes containing flowing fluids, and high speed magnetic and paper tapes. The dynamic behavior of a telescopically moving beam has been studied. Tabarrok et al. (1974) utilized the conservation of momenta and continuity equations to derive the equations of motion of an axially moving beam whose length changes with time. Their model resulted in four non-linear partial differential equations and one algebraic equation. With the assumption of small deformation gradients and constant tension, those equations were reduced to one partial differential equation. A procedure was also described for obtaining approximate solutions for various axial velocities of the beam. Wang and Wei (1987) used Newton's approach in deriving the governing equation of an axially moving beam, and utilized the Galerkin's approximation technique in discretizing the elastic displacements. They found that the extending and contraction motions of the beam have destabilizing and stabilizing effects on the vibratory motions, respectively. Yuh and Young (1991) used Newton's approach to derive a time-varying partial differential equation and boundary conditions for an axially moving beam with rotation. An approximated model was derived by using the assumed mode method and the validity of the approximated model was investigated by experiment. Stylianou and Tabarrok (1994) used the finite element method and obtained the response and stability of an axially moving beam problem. A variable-domain beam finite element the size of which is a prescribed function of time was formulated.

Fung et al. (1998) applied Hamilton's principle to derive non-linear partial differential equations of an axially moving beam with a tip mass. Four models including Timoshenko, Euler, simple-flexible and rigid-body beam theories were proposed and discussed. Oz and Pakdemirli (1999) investigated the

dynamic response of an axially accelerating, elastic, tensioned beam. The time-dependent velocity was assumed to vary harmonically about a constant mean velocity. It was found that instabilities occur when the frequency of velocity fluctuations is close to two times the natural frequency of the constant velocity system or when the frequency is close to the sum of any two natural frequencies. Ozkaya and Pakdemirli (2000) studied transverse vibrations of an axially moving beam. The method of matched asymptotic expansions and the method of multiple scales were applied to solve the problem. All solutions were non-resonant solutions. Oz et al. (2001) studied non-linear vibration and stability of an axially moving beam with harmonically varying velocity. The method of multiple scales was used in search of approximate solutions. Ozkaya and Oz (2002) used artificial neural networks method to determine the natural frequencies and stability regions of an axially moving beam.

Lee et al. (2004) formulated the spectral element model for an axially moving Timoshenko beam under a uniform axial tension. The effects of the axial velocity and axial tension on the vibration characteristics, the dispersion relation and the stability were investigated. Sze et al. (2005) employed Galerkin method to discretize the governing equations of an axially moving beam and formulated the incremental harmonic balance method for non-linear vibration. Cepon and Boltezar (2007) applied an approximate Galerkin finite-element method to solve the initial-/boundary-value problem of a viscously damped and axially moving beam with pre-tension. It was shown that for certain values of the parameters, especially at high velocities, Galerkin method using stationary string eigenfunctions would give a poor prediction of the dynamic response. Lin and Qiao (2008) investigated vibration and stability for an axially moving beam in fluid and constrained by simple supports with torsion springs. The effects of axially moving speed, axial added mass coefficient, and several other system parameters on the dynamics and instability of the beam were discussed. It was shown that when the moving speed exceeds a certain value, the beam is subject to buckling-type instability. Piovan and Sampaio (2008) developed a formulation for axially moving beams made of functionally graded materials. The variation of properties along the wall thickness of the annular cross-section follows a simple exponential law. The simulation results showed that a beam in which the ceramic is the main component has a high oscillatory deployment but when the beam has a metallic main component the frequency of oscillation is lower.

Chang et al. (2010) investigated the vibration and stability of an axially moving beam. The effects of oscillation amplitude and frequency of periodical axial movement on the stability of the beam were discussed from the stability chart. Time histories

were established to confirm the results from Floquet theory. Ghayesh and Amabili (2013) also investigated the non-linear dynamics of an axially moving beam with time-dependent axial speed, whereas the non-linear partial differential equation of motion was discretized and reduced to a set of ordinary differential equations. Banerjee and Jackson (2013) developed a rotating tapered Rayleigh beam for investigating its free vibration characteristics. The dynamic stiffness matrix and Wittrick-Williams algorithm were applied to illustrate the natural frequencies and mode shape. Zhu and Chung (2016) proposed a spinning beam which is established in an inertial reference frame by using Rayleigh beam theory. Arvin (2017) developed a micro rotating Timoshenko and Euler-Bernoulli beam based on the strain gradient theory. The flapping and axial natural frequencies were solved by using the differential transform method. Yang et al. (2018) developed a beam which considered bi-gyroscopic continua as a prototype. The influence of bi-gyroscopic effects on the natural frequencies, modes, and stability was investigated under the axially moving and spinning beam. Zhu and Chung (2019) developed a simply supported beam that has spinning speed and axially moving motion. The natural frequencies based on Rayleigh beam theory were investigated and compared to those of the previous studies.

In previous studies, most researchers on stability analysis are only for beams with uniform speed of extension and retraction. In this paper, the equations of motion of an axially moving and spinning beam are derived by using Hamilton's principle and the finite element method with time-varying length of element. Two kinds of axial motion including constant-speed extension deployment and back-and-forth periodical motion are investigated. The eigenvalues of equations of motion are obtained to determine the stability of a moving beam with constant-speed axial extension deployment. Floquet theory is employed to investigate the dynamic stability of a telescopically moving beam with time-dependent velocity. The effect of the spinning speed of the beam on its stability is studied. Direct time numerical integration, based on a Runge-Kutta algorithm, is used to confirm the results from Floquet theory.

## THEORY AND FORMULATION

The physical configuration of an axially moving and spinning system is shown in Figure 1. The beam is modeled by using Rayleigh beam theory in which the effect of rotary inertia is taken into account. Because of the coupling of the spinning and the lateral rotation, the gyroscopic effect is included in this model. The left part of the beam inside the wall has no deflection since the wall is assumed to be rigid. An axial load,  $P$ , is applied at the left end of the

beam to drive the axial motion of the beam. The beam has an axial motion and its deflection can be described by transverse and rotational displacements based on Rayleigh beam model. The beam under consideration spins about and moves along its longitudinal axis. A fixed coordinate system ( $XYZ$ ) is defined with the  $X$ -axis along the undeformed longitudinal axis of the beam and the unit vectors along the  $X$ ,  $Y$  and  $Z$ -axes are denoted as  $\mathbf{i}$ ,  $\mathbf{j}$  and  $\mathbf{k}$ , respectively. A rotating coordinate system ( $xyz$ ) is defined to be attached on the spinning beam and its unit vectors are denoted as  $\mathbf{i}'$ ,  $\mathbf{j}'$  and  $\mathbf{k}'$ , respectively. The  $x$ - and  $X$ -axes coincide. The angle between the  $\mathbf{j}$  and  $\mathbf{j}'$  unit vectors is given by  $\Omega t$ , where  $\Omega t$  is the constant spin speed of the beam.

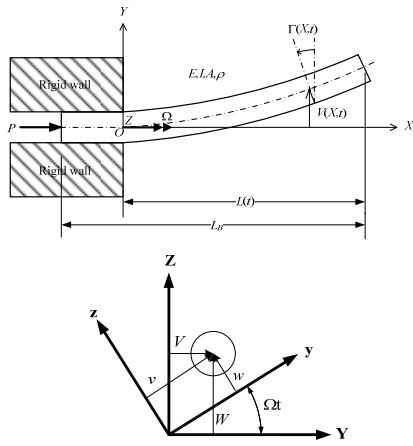


Fig. 1. Schematic of an axially moving and spinning beam system.

### Finite element discretization

The position vector of any material point ( $x(t)$ ,  $y$ ,  $z$ ) of an axially moving and spinning Rayleigh beam before deformation is

$$\mathbf{r}' = x(t)\mathbf{i}' + y\mathbf{j}' + z\mathbf{k}'. \quad (1)$$

The displacement field of the Rayleigh beam is

$$\mathbf{U}' = [-y\gamma(x(t), t) + z\beta(x(t), t)]\mathbf{i}' + v(x(t), t)\mathbf{j}' + w(x(t), t)\mathbf{k}'. \quad (2)$$

where  $v(x(t), t)$  and  $w(x(t), t)$  represent the transverse displacements along the  $y$  and  $z$  directions, respectively, and  $\beta(x(t), t)$  and  $\gamma(x(t), t)$  represent the rotational displacements with respect to the  $y$  and  $z$  axes, respectively.

The position vector of the point ( $x(t)$ ,  $y$ ,  $z$ ) after deformation is

$$\mathbf{R}' = \mathbf{r}' + \mathbf{U}' = [x(t) - y\gamma(x(t), t) + z\beta(x(t), t)]\mathbf{i}' + [y + v(x(t), t)]\mathbf{j}' + [z + w(x(t), t)]\mathbf{k}'. \quad (3)$$

Taking total derivative of  $\mathbf{R}'$  with respect to time, we obtain the velocity of this point

$$\frac{D\mathbf{R}'}{Dt} = [\dot{x} - y(\gamma_{,x}\dot{x} + \dot{\gamma}) + z(\beta_{,x}\dot{x} + \dot{\beta})]\mathbf{i}' + [(v_{,x}\dot{x} + \dot{v} - w\Omega) - z\Omega]\mathbf{j}' + [(w_{,x}\dot{x} + \dot{w} + v\Omega) + y\Omega]\mathbf{k}'. \quad (4)$$

where the subscript preceded by a comma denotes partial differentiation with respect to that subscript.

The kinetic energy  $K_E$  of the axially moving and spinning Rayleigh beam is

$$K_E = \frac{1}{2}\rho A \int_0^{L(t)} \dot{x}^2 dx + \frac{1}{2}\rho A \int_0^{L(t)} [(v_{,x}\dot{x} + \dot{v} - w\Omega)^2 + (w_{,x}\dot{x} + \dot{w} + v\Omega)^2] dx + \frac{1}{2}\rho I \int_0^{L(t)} [(\gamma_{,x}\dot{x} + \dot{\gamma})^2 + (\beta_{,x}\dot{x} + \dot{\beta})^2 + 2\Omega^2] dx. \quad (5)$$

The elastic strain energy  $S_E$  of the Rayleigh beam due to bending is

$$S_E = \frac{1}{2}EI \int_0^{L(t)} (v_{,xx}^2 + w_{,xx}^2) dx. \quad (6)$$

The potential energy due to the axial inertia force  $U_a$  is

$$U_a = -\frac{1}{2}\rho A \int_0^{L(t)} (L-x)\ddot{x}(v_{,x}^2 + w_{,x}^2) dx. \quad (7)$$

Neglecting the axial deformation of the beam, one has  $\dot{x} = \dot{L}$  and  $\ddot{x} = \ddot{L}$ , and the kinetic energy  $K_E$  and the potential energy  $U_a$  can be rewritten as

$$K_E = \frac{1}{2}\rho A \int_0^{L(t)} \dot{L}^2 dx + \frac{1}{2}\rho A \int_0^{L(t)} [(v_{,x}\dot{L} + \dot{v} - w\Omega)^2 + (w_{,x}\dot{L} + \dot{w} + v\Omega)^2] dx + \frac{1}{2}\rho I \int_0^{L(t)} [(\gamma_{,x}\dot{L} + \dot{\gamma})^2 + (\beta_{,x}\dot{L} + \dot{\beta})^2 + 2\Omega^2] dx, \quad (8)$$

$$U_a = -\frac{1}{2}\rho A \int_0^{L(t)} (L-x)\ddot{L}(v_{,x}^2 + w_{,x}^2) dx. \quad (9)$$

By using the variable-domain element, the protruded beam is divided into  $n$  elements of equal length,  $l(t) = L(t)/n$ . Each element consists of two nodes; each node has the degrees of freedom of transverse and rotational displacements. The kinetic energy  $K_{Ei}$ , the strain energy  $S_{Ei}$  and the potential energy due to axial inertia force  $U_{ai}$  of the  $i$ th beam element are then given by, respectively,

$$K_{Ei} = \frac{1}{2}\rho A \int_0^{l(t)} [(v_{e,s}\dot{s} + \dot{v}_e - w_e\Omega)^2 + (w_{e,s}\dot{s} + \dot{w}_e + v_e\Omega)^2] ds + \frac{1}{2}\rho I \int_0^{l(t)} [(\gamma_{e,s}\dot{s} + \dot{\gamma}_e)^2 + (\beta_{e,s}\dot{s} + \dot{\beta}_e)^2 + 2\Omega^2] ds + \frac{1}{2}\rho A l \dot{L}^2, \quad (10)$$

$$S_{Ei} = \frac{1}{2}EI \int_0^{l(t)} (v_{e,ss}^2 + w_{e,ss}^2) ds, \quad (11)$$

$$U_{ai} = -\frac{1}{2}\rho A \int_0^{l(t)} (L-L_i-s)\ddot{L}(v_{e,s}^2 + w_{e,s}^2) ds. \quad (12)$$

where  $s$  refers to the element coordinate system (ECS),  $(v_e, w_e)$  and  $(\beta_e, \gamma_e)$  are, respectively, the transverse and rotational displacements corresponding to the ECS, and  $L_i$  locates the ECS, as shown in Figure 2. Here we introduce a new parameter  $di$  defined for each element as

$$d_i = L - L_i = L \left( 1 - \frac{i-1}{n} \right), \quad i = 1, 2, \dots, n. \quad (13)$$

By using the above definition, the expressions for the energies of the  $i$ th element become

$$K_{Ei} = \frac{1}{2} \rho A \int_0^{l(t)} \left[ (v_{e,s} \dot{d}_i + \dot{v}_e - w_{e,s} \Omega)^2 + (w_{e,s} \dot{d}_i + \dot{w}_e + v_e \Omega)^2 \right] ds \quad (14)$$

$$+ \frac{1}{2} \rho I \int_0^{l(t)} \left[ (\gamma_{e,s} \dot{d}_i + \dot{\gamma}_e)^2 + (\beta_{e,s} \dot{d}_i + \dot{\beta}_e)^2 + 2\Omega^2 \right] ds + \frac{1}{2} \rho A l \dot{L}^2,$$

$$S_{Ei} = \frac{1}{2} EI \int_0^{l(t)} (v_{e,ss}^2 + w_{e,ss}^2) ds, \quad (15)$$

$$U_{ai} = -\frac{1}{2} \rho A \int_0^{l(t)} (d_i - s) \ddot{L} (v_{e,s}^2 + w_{e,s}^2) ds. \quad (16)$$

Displacements in the fixed coordinate system ( $XYZ$ ) and in the rotating coordinate system ( $xyz$ ) are related as

$$\begin{Bmatrix} v_e \\ w_e \end{Bmatrix} = \begin{bmatrix} \cos \Omega t & \sin \Omega t \\ -\sin \Omega t & \cos \Omega t \end{bmatrix} \begin{Bmatrix} V_e \\ W_e \end{Bmatrix}, \quad (17)$$

$$\begin{Bmatrix} \beta_e \\ \gamma_e \end{Bmatrix} = \begin{bmatrix} \cos \Omega t & \sin \Omega t \\ -\sin \Omega t & \cos \Omega t \end{bmatrix} \begin{Bmatrix} B_e \\ \Gamma_e \end{Bmatrix}. \quad (18)$$

where  $V_e$  and  $W_e$  are the transverse displacements along the  $Y$  and  $Z$  axes, respectively, and  $B_e$  and  $\Gamma_e$  are the rotational displacements with respect to the  $Y$  and  $Z$  axes, respectively.

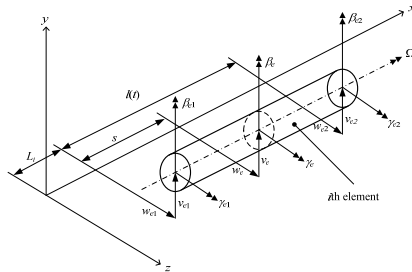


Fig. 2. Element coordinate system (ECS).

With Eqs. (17) and (18), the energies of the  $i$ th element become

$$K_{Ei} = \frac{1}{2} \rho A \int_0^{l(t)} \left[ (V_{e,s} \dot{d}_i + \dot{V}_e)^2 + (W_{e,s} \dot{d}_i + \dot{W}_e)^2 \right] ds \quad (19)$$

$$+ \frac{1}{2} \rho I \int_0^{l(t)} \left[ (\Gamma_{e,s} \dot{d}_i + \dot{\Gamma}_e)^2 + (B_{e,s} \dot{d}_i + \dot{B}_e)^2 \right] ds$$

$$+ \rho I \Omega \int_0^{l(t)} \left[ \Gamma_e \dot{B}_e - \dot{\Gamma}_e B_e + \dot{d}_i (\Gamma_e B_{e,s} - \Gamma_{e,s} B_e) \right] ds$$

$$+ \frac{1}{2} \rho A l \dot{L}^2 + \rho I \Omega^2,$$

$$S_{Ei} = \frac{1}{2} EI \int_0^{l(t)} (V_{e,ss}^2 + W_{e,ss}^2) ds, \quad (20)$$

$$U_{ai} = -\frac{1}{2} \rho A \int_0^{l(t)} (d_i - s) \ddot{L} (V_{e,s}^2 + W_{e,s}^2) ds. \quad (21)$$

The displacements ( $V_e$ ,  $W_e$ ,  $B_e$ ,  $\Gamma_e$ ) of a typical point within the element can be expressed in terms of the nodal displacement vector  $\{q_e\}$  and shape functions,  $[N_V]$ ,  $[N_W]$ ,  $[N_B]$  and  $[N_\Gamma]$  (Nelson and McVaugh (1976))

Upon substituting Eqs. (19-21) into Lagrange's equation, the equations of motion for the beam element are given as

$$[M_e] \{\ddot{q}_e\} + [C_e] \{\dot{q}_e\} + [K_e] \{q_e\} = \{0\}. \quad (22)$$

where  $[M_e]$ ,  $[C_e]$ , and  $[K_e]$  are the element mass, damping and stiffness matrices, respectively, and all are time-dependent.

### System equations of motion

The equations of motion for the whole system can be obtained by assembling the element equations, and take the following well-known form

$$[M] \{\ddot{q}\} + [C] \{\dot{q}\} + [K] \{q\} = \{0\}. \quad (23)$$

where

$$[M] = \sum_{e=1}^n [M_e], \quad [C] = \sum_{e=1}^n [C_e], \quad (24)$$

$$[K] = \sum_{e=1}^n [K_e], \quad \{q\} = \sum_{e=1}^n \{q_e\}.$$

$\{q\}$  is the overall displacement vector;  $[M]$ ,  $[C]$ , and  $[K]$  are the overall mass, damping and stiffness matrices, respectively. The boundary conditions associated with Eq. (23) are  $V(0, t) = 0$ ,  $V_{,x}(0, t) = 0$ ,  $V_{,xx}(L, t) = 0$ ,  $V_{,xxx}(L, t) = 0$ ,  $W(0, t) = 0$ ,  $W_{,x}(0, t) = 0$ ,  $W_{,xx}(L, t) = 0$  and  $W_{,xxx}(L, t) = 0$ . The vibration analysis including natural frequencies and transient response of the beam can be performed by solving Eq. (23).

## STABILITY ANALYSIS

The stability of the beam with two kinds of axial motion including constant-speed extension deployment and back-and-forth periodical motion is investigated. For beams with constant-speed extension deployment, stability is determined by the real and imaginary parts of the eigenvalues of the equations of motion. However, the eigenvalues for beams with periodical axial motion are alternating with time, and therefore cannot be used to determine the stability of beams with this type of motion. The stability for beams with periodical axial motion will be analyzed by using Floquet theory.

### Stability analysis by eigenvalues

The governing Eq. (23) is reduced to a set of first-order differential equations as

$$\{\dot{z}\} = [D]\{z\}. \quad (25)$$

where

$$\{z\} = \begin{Bmatrix} \{\dot{q}\} \\ \{q\} \end{Bmatrix}, [D] = \begin{bmatrix} -[M]^{-1}[C] & -[M]^{-1}[K] \\ [I] & [0] \end{bmatrix}. \quad (26)$$

where  $[I]$  is the identity matrix and  $\{z\}$  is a column vector with the components  $z_i, i=1, 2, \dots, j$ , where  $j = 4n$ . To calculate the eigenvalues of the system,  $\{z\}$  is assumed to be

$$\{z\} = \{A\} e^{\lambda t}. \quad (27)$$

where  $\lambda$  is generally complex and  $\{A\}$  is a constant vector. The reduced Eq. (25) eventually leads to the eigenvalue problem

$$(\lambda[I] - [D])\{A\} = \{0\}. \quad (28)$$

Since the axial-motion profile is given for evaluation of  $[D]$ , we only proceed with the solution of the conventional eigenvalue problem. The real and imaginary parts of the eigenvalues are related to the damping coefficients and the vibration frequencies, respectively. The type of stability can be determined from the signs of the real and imaginary parts of eigenvalue as follows:

1. The system is stable if all  $\text{Re}(\lambda) \leq 0$ .
2. The system is dynamic instable (flutter) if at least one  $\text{Re}(\lambda) > 0$  and its corresponding  $\text{Im}(\lambda) \neq 0$ .
3. The system is static instable (divergence) if at least one  $\text{Re}(\lambda) > 0$  and its corresponding  $\text{Im}(\lambda) = 0$ .

Since the eigenvalue  $\lambda_i$  is time-dependent,  $\lambda_i$  over a long period of time is needed to determine stability of beams with constant-speed axial extension deployment. However, for beams with back-and-forth periodic axial motion, the eigenvalues are alternating about the critical value, 0, so the determination of the stability using eigenvalues method for such problems fails.

### Stability analysis by Floquet theory

When the system is linear and the time-dependent coefficients of the equations of motion are periodic, a stability analysis can be performed by Floquet theory as explained by Nayfeh and Mook (1979).

The length of the beam is prescribed to be a periodic function of time with period  $T$  and the matrix  $[D]$  also varies periodically with period  $T$ . The linear system expressed by Eq. (25) admits a set of linearly independent solutions,  $z_{1i}(t), z_{2i}(t), \dots, z_{ji}(t)$  with  $i = 1, 2, \dots, j$ , which constitute the fundamental set of solutions,  $[Z(t)]$ . Clearly  $[Z(t)]$  satisfies the

matrix equation

$$[\dot{Z}(t)] = [D(t)][Z(t)]. \quad (29)$$

Due to the periodic nature of  $[M]$ ,  $[C]$  and  $[K]$ , it is deduced that  $[D(t+T)] = [D(t)]$  and  $[Z(t+T)]$  also forms a fundamental set of solutions. A relation can be established as

$$[Z(t+T)] = [\Phi][Z(t)]. \quad (30)$$

where  $[\Phi]$  is termed as the Floquet transition matrix (FTM), which provides the stability condition through an eigen-analysis procedure.  $[\Phi]$  is obtained numerically. By setting  $[Z(0)] = [I]$ , it is seen from Eq. (30) that  $[Z(T)] = [\Phi]$ . This means that  $[\Phi]$  is equal to  $[Z(T)]$  when the system is solved with initial conditions  $[Z(0)] = [I]$ . The eigenvalues of the FTM,  $\lambda_i$ , are called the Floquet or characteristic multipliers and the stable condition can be expressed as

$$|\lambda_i| \leq 1, \quad i = 1, 2, \dots, 4n. \quad (31)$$

## NUMERICAL RESULTS AND DISCUSSION

Runge–Kutta algorithm is used to integrate the governing equations of the beam. Since this paper is a continuation of the study, the verification part has been verified in the previous study. The present results for the tip displacement of the beam of linear extrusion and retraction with various speeds corresponding to the four simulations are shown in Figure 3 and Figure 4 of the Chang et al. (2010). Good agreements are achieved in all four test cases.

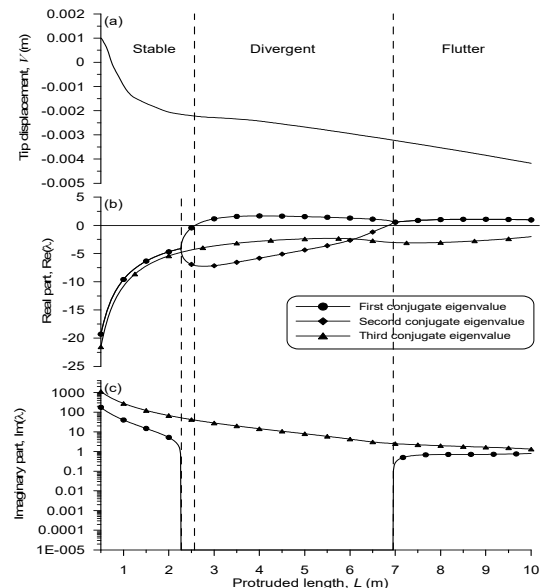


Fig. 3. Variation of (a) tip response, (b) real parts (c) and imaginary parts of the first three conjugate eigenvalues with  $L(t) = 0.5+20t$  m and  $\Omega = 0$  rad/s.

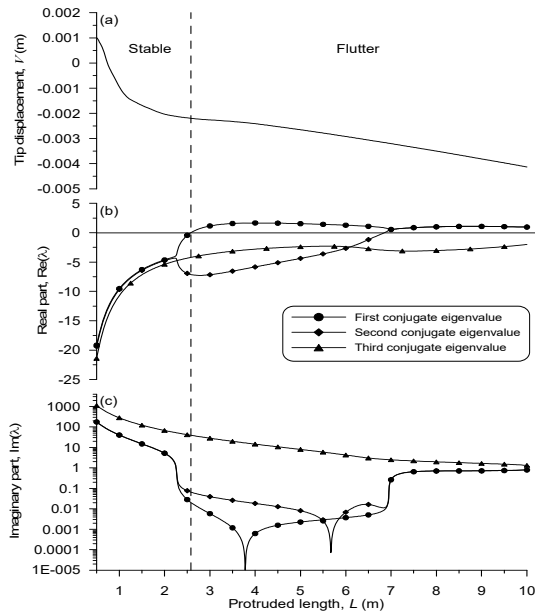


Fig. 4. Variation of (a) tip response, (b) real parts (c) and imaginary parts of the first three conjugate eigenvalues with  $L(t) = 0.5 + 20t$  m and  $\Omega = 5000$  rad/s.

*Vibration and Stability of Beams with Constant-speed Axial Extension Deployment*

In the following subsections, the cross section of the beam is circular with a radius of 0.005 m; the mass density is 2710 kg/m<sup>3</sup> and Young’s modulus is 71.0 GPa. The initial tip displacement of the beam is assumed to be 0.001 m for all cases studied. The variation of tip response and real and imaginary parts of the first three conjugate eigenvalues for various extension-deployment speeds,  $L_t = 20$  m/s, and different spin speeds,  $\Omega = 0, 5000, 10000$  rad/s, are illustrated in Figures 3-5. Fig. 3 ( $L_t = 20$  m/s,  $\Omega = 0$  rad/s) shows that the beam experiences three stages of response, stable, divergent and flutter, with an increasing protruded length. In Figure 4 ( $L_t = 20$  m/s,  $\Omega = 5000$  rad/s) and Figure 5 ( $L_t = 20$  m/s,  $\Omega = 10000$  rad/s), the beam experiences only two stages of response, stable and flutter, with an increasing protruded length. The stage of divergence does not appear because the imaginary part of the eigenvalue is above zero in the range of protruded length studied. By comparing Figs. 3b, 4b and 5b, it is found that the real part of the first conjugate eigenvalue changes from negative to positive at the same protruded length.

The transient responses of the tip of the beam with constant-speed extension rate and different spin speeds are illustrated in Figure 6. The spin speeds of the beam are set to 0, 5000 and 10000 rad/s and the length functions of the beam are  $L(t) = 0.5 + 20t$ ,  $L(t) = 0.5 + 10t$  and  $L(t) = 0.5 + 5t$  m. It is observed that the vibration amplitude of the transient response is suppressed due to the spinning of the beam. For higher spin speed, the effect of suppression is more

significant.

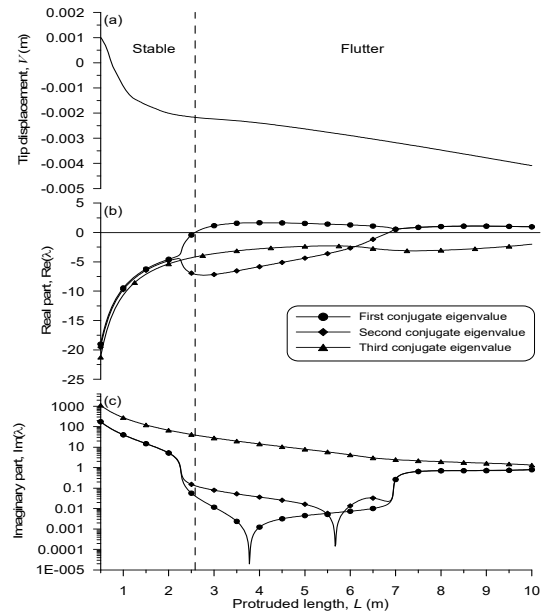


Fig. 5. Variation of (a) tip response, (b) real parts (c) and imaginary parts of the first three conjugate eigenvalues with  $L(t) = 0.5 + 20t$  m and  $\Omega = 10000$  rad/s.

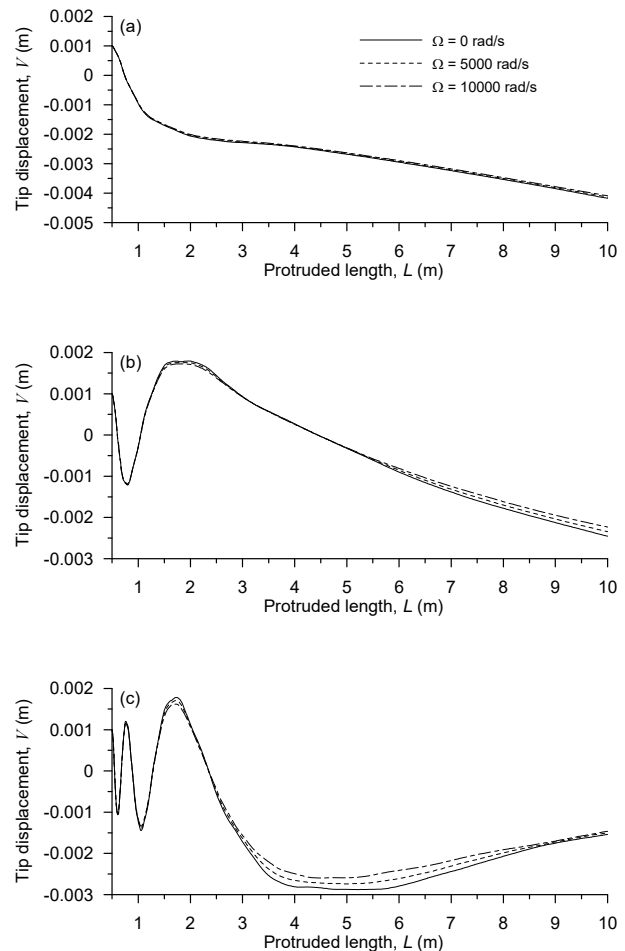


Fig. 6. Tip responses of the beam with (a)  $L(t) = 0.5 + 20t$  m, (b)  $L(t) = 0.5 + 10t$  m, and (c)  $L(t) = 0.5 + 5t$  m, and  $\Omega = 0, 5000, 10000$  rad/s.

*Vibration and Stability of Beams with with Periodical Axial Motion*

In this subsection, Floquet theory is applied to study the stability of a system translating with a periodical axial motion and spinning with constant speed. The length function of the beam for simulations is given by

$$L(t) = 0.5 + L_a \sin(\omega_a t) \text{ (m)} \quad (25)$$

where  $L_a$  and  $\omega_a$  represent the amplitude and frequency of the periodical axial motion of the beam, respectively. The axial-oscillation amplitude is varied from 0 to 0.01 m. The Campbell diagram of the spinning beam with a fixed length  $L = 0.5$  m is shown in Figure 7. The first three natural frequencies of the beam obtained are  $\omega_1=180.0$ ,  $\omega_2=1127$ , and  $\omega_3 = 3156$  rad/s. It is observed that the whirl speeds of the Euler beam remain the same while the spin speed increases. When the beam is modeled as a Rayleigh beam, the whirl speeds bifurcate when the spin speed increases. This is due to the effects of gyroscopic moment and rotary inertia. The first three forward and backward whirl speeds at  $\Omega = 10000$  rad/s are  $\omega_{1F} = 181.1$ ,  $\omega_{2F} = 1136$ ,  $\omega_{3F} = 3175$ ,  $\omega_{1B} = 178.8$ ,  $\omega_{2B} = 1119$ , and  $\omega_{3B} = 3137$  rad/s. The regions of dynamic instability for the present system with  $\Omega = 0, 5000, 10000$  rad/s are shown in Figures 8 and 9.

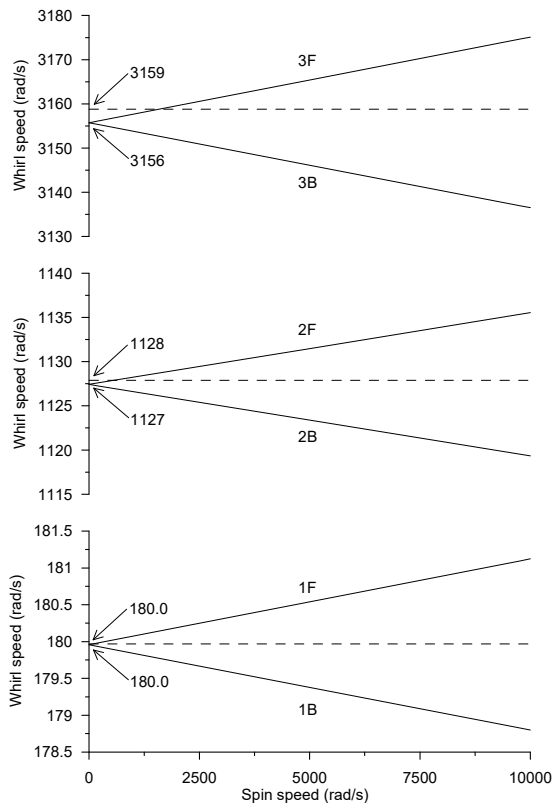


Fig. 7. Campbell diagram of the cantilevered spinning beam with  $L(t) = 0.5$  m. — Rayleigh beam model; - - - Euler beam model.

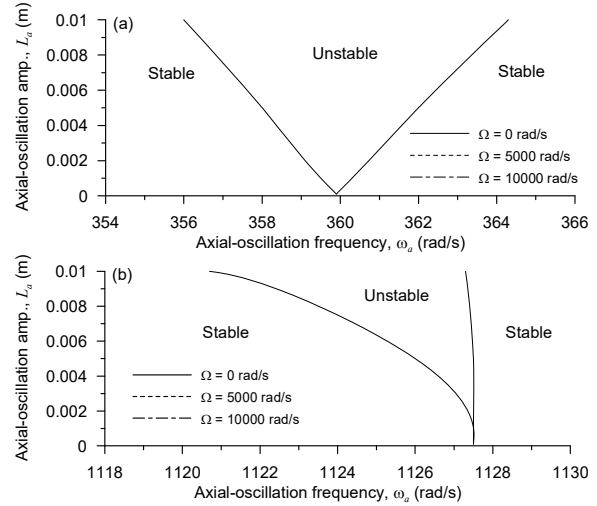


Fig. 8. The stable and unstable regions near (a)  $2\omega_1$  and (b)  $\omega_2$  with  $L(t) = 0.5 + L_a \sin(\omega_a t)$  m and  $\Omega = 0, 5000, 10000$  rad/s.

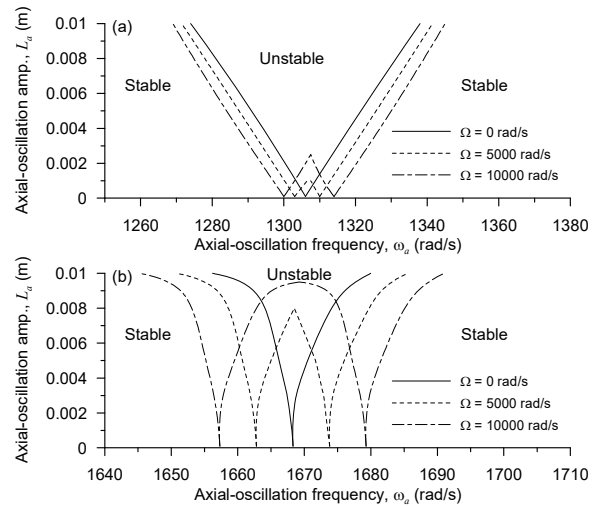


Fig. 9. The stable and unstable regions near (a)  $\omega_1 + \omega_2$  and (b)  $(\omega_1 + \omega_3)/2$  with  $L(t) = 0.5 + L_a \sin(\omega_a t)$  m and  $\Omega = 0, 5000, 10000$  rad/s.

Unstable regions occur at axial-oscillation frequencies of about 360.0, 1127, 1307, 1668 etc rad/s, which are observed to be near the linear combination of the natural frequencies  $2\omega_1$ ,  $\omega_2$ ,  $\omega_1 + \omega_2$ ,  $(\omega_1 + \omega_3)/2$  etc. It is observed that as the spin speed increases, the boundaries of the regions of dynamic instability near  $2\omega_1$  and  $\omega_2$  are almost unchanged but those near  $\omega_1 + \omega_2$  and  $(\omega_1 + \omega_3)/2$  are changed from V-shaped to W-shaped. The widths of the unstable regions increase as the axial-oscillation amplitude increases, therefore, the system becomes more unstable. It may be concluded that the unstable regions near the multiples of individual natural frequencies,  $2\omega_1$  and  $\omega_2$ , are spin-speed independent and those near the

combination of multiple natural frequencies,  $\omega_1 + \omega_2$  and  $(\omega_1 + \omega_3)/2$  are spin-speed dependent.

Figure 10 shows the transient response of the tip displacement for different spin speeds. Good agreements are observed with the prediction from Floquet theory. Indeed, Fig. 10a ( $\omega_a=1340$  rad/s,  $L_a=0.01$  m and  $\Omega=0$  rad/s) shows the transient response that was predicted to be stable. It also shows that even after many periods the amplitude of tip displacement remains bounded, therefore this system is confirmed to be stable. Fig. 10b ( $\omega_a=1340$  rad/s,  $L_a=0.01$  m and  $\Omega=5000$  rad/s) and Fig. 10c ( $\omega_a=1340$  rad/s,  $L_a=0.01$  m and  $\Omega=10000$  rad/s) show that the amplitude of tip displacement increases periodically. The amplitude of the tip displacement with  $\Omega=10000$  rad/s is larger than that with  $\Omega=5000$  rad/s. This confirms the nature of the beam with corresponding parameter set, which was already recognized to be unstable in the previous Floquet analysis shown in Fig. 9.

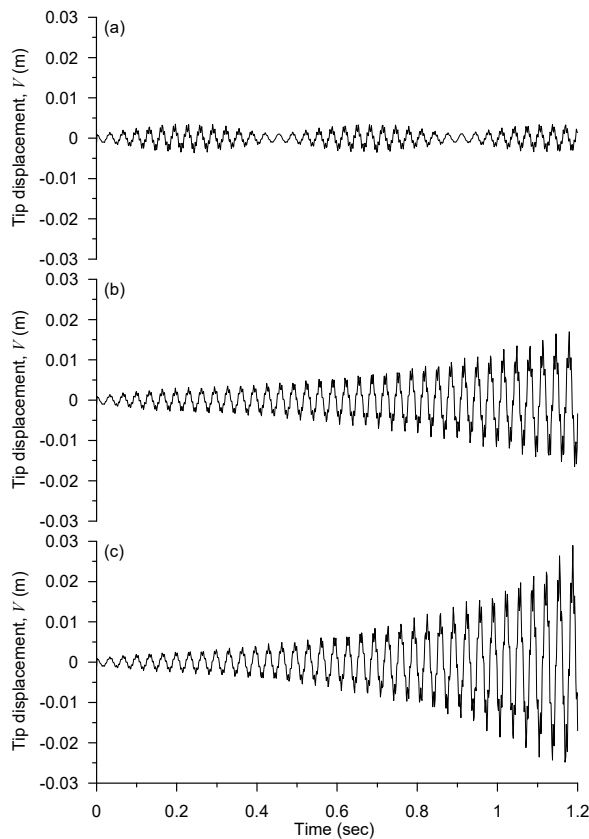


Fig. 10. Transient response of tip of the beam with  $L(t)=0.5+0.01 \sin(1340t)$  m and different spin speeds. (a)  $\Omega=0$ , (b)  $\Omega=5000$ , (c)  $\Omega=10000$  rad/s.

**Conclusions**

The equations of motion of an axially moving and spinning Rayleigh beam are derived by using Hamilton’s principle and the finite element method

with variable-domain element. The effect of spin suppresses the amplitude of the transient response of the beam with constant-speed extension deployment. However, the protruded length of the beam at which flutter occurs is spin-speed independent. The dynamic stability of a beam with periodical axial motion and different spin speeds is investigated by using Floquet theory. It is found that as the spin speed of the beam increases, the boundaries of unstable regions of the system near  $2\omega_1$  and  $\omega_2$  are almost unchanged but those near  $\omega_1 + \omega_2$  and  $(\omega_1 + \omega_3)/2$  are changed from V-shaped to W-shaped. It may be concluded that the unstable regions near the multiples of individual natural frequencies,  $2\omega_1$  and  $\omega_2$ , are spin-speed independent and those near the linear combination of multiple natural frequencies,  $\omega_1 + \omega_2$  and  $(\omega_1 + \omega_3)/2$  are spin-speed dependent. Finally the transient responses of the spinning beam with periodical axial motion near  $\omega_1 + \omega_2$  are obtained and the results of stability analysis by using Floquet theory are confirmed.

**REFERENCES**

Arvin, H., “Free vibration analysis of micro rotating beams based on the strain gradient theory using the differential transform method: Timoshenko versus Euler-Bernoulli beam models,” *European Journal of Mechanics A/Solids*, Vol. 65, pp. 336-348 (2017).

Banerjee, J. R., Jackson, D. R., “Free vibration of a rotating tapered Rayleigh beam: A dynamic stiffness method of solution,” *Computers and Structures*, Vol. 124, pp. 11-20 (2013).

Cepon, G., Boltezar, M., “Computing the dynamic response of an axially moving continuum,” *Journal of Sound and Vibration*, Vol. 300, pp. 316-329 (2007).

Chang, J. R., Lin, W. J., Huang, C. J., Choi, S. T., “Vibration and stability of an axially moving Rayleigh beam,” *Applied Mathematical Modelling*, Vol. 34, pp. 1482-1497 (2010).

Fung, R. F., Lu, P. Y., Tseng, C. C., “Non-linearly dynamic modeling of an axially moving beam with a tip mass,” *Journal of Sound and Vibration*, Vol. 218(4), pp. 559-571 (1998).

Ghayesh, M. H., Amabili, M., “Steady-state transverse response of an axially moving beam with time-dependent axial speed,” *International Journal of Non-Linear Mechanics*, Vol. 49, pp. 40-49 (2013).

Lin, W., Qiao, N., “Vibration and stability of an axially moving beam immersed in fluid,” *Solids and Structures*, Vol. 45, pp. 1445-1457 (2008).

- Lee, U., Kim, J., Oh, H., "Spectral analysis for the transverse vibration of an axially moving Timoshenko beam," *Journal of Sound and Vibration*, Vol. 271, pp. 685-703 (2004).
- Mote Jr., C. D., "Dynamic stability of axially moving materials," *The Shock and Vibration Digest*, Vol. 14(4), pp. 2-11 (1972).
- Nayfeh, A. H., Mook, D., *Nonlinear Oscillations*, Wiley, New York, 1979.
- Nelson, H. D., McVaugh, J. M., "The Dynamics of Rotor-Bearing Systems Using Finite Elements," *Journal of Engineering for Industry*, Vol. 98(2), pp. 593-600 (1976).
- Ozkaya, E., Pakdemirli, M., "Vibrations of an axially accelerating beam with small flexural stiffness," *Journal of Sound and Vibration*, Vol. 234(3), pp. 521-535 (2000).
- Ozkaya, E., Oz, H. R., "Determination of natural frequencies and stability regions of axially moving beams using artificial neural networks method," *Journal of Sound and Vibration*, Vol. 252(4), pp. 782-789 (2002).
- Oz, H. R., Pakdemirli, M., "Vibrations of an axially moving beam with time-dependent velocity," *Journal of Sound and Vibration*, Vol. 227(2), pp. 239-257 (1999).
- Oz, H. R., Pakdemirli, M., Boyaci, H., "Non-linear vibrations and stability of axially moving beam with time-dependent velocity," *International Journal of Non-Linear Mechanics*, Vol. 36, pp. 107-115 (2001).
- Piovan, M. T., Sampaio, R., "Vibrations of axially moving flexible beams made of functionally graded materials," *Thin-Walled Structures*, Vol. 46, pp. 112-121 (2008).
- Stylianou, M., Tabarrok, B., "Finite element analysis of an axially moving beam, part I: time integration," *Journal of Sound and Vibration*, Vol. 178(4), pp. 433-453 (1994).
- Stylianou, M., Tabarrok, B., "Finite element analysis of an axially moving beam, part II: stability analysis," *Journal of Sound and Vibration*, Vol. 178(4), pp. 455-481 (1994).
- Sze, K. Y., Chen, S. H., Huang, J. L., "The incremental harmonic balance method for nonlinear vibration of axially moving beams," *Journal of Sound and Vibration*, Vol. 281, pp. 611-626 (2005).
- Tabarrok, B., Leech, C. M., Kim, Y. I., "On the dynamics of an axially moving beam," *Journal of Franklin Institute: Engineering and Applied Mathematics*, Vol. 297 (3), pp. 201-220 (1974).
- Wang, P. K. C., Wei, J. D., "Vibrations in a moving flexible robot arm," *Journal of Sound and Vibration*, Vol. 116(1), pp. 149-160 (1987).
- Yuh, J., Young, T., "Dynamics modeling of an axially moving beam in rotation: simulation and experiment," *Journal of Dynamic Systems, Measurement, and Control*, Vol. 113, pp. 34-40 (1991).
- Yang, X. D., Yang, J. H., Qian, Y. J., Zhang, W., Melnik, V. N., "Dynamics of a beam with both axial moving and spinning motion: An example of bi-gyroscopic continua," *European Journal of Mechanics A/Solids*, Vol. 69, pp. 231-237 (2018).
- Zhu, K., Chung, J., "Dynamic modeling and analysis of a spinning Rayleigh beam under deployment," *International Journal of Mechanical Sciences*, Vol. 115-116, pp. 392-405 (2016).
- Zhu, K., Chung, J., "Vibration and stability analysis of a simply-supported Rayleigh beam with spinning and axial motions," *Applied Mathematical Modelling*, Vol. 66, pp. 362-382 (2019).

## NOMENCLATURE

$A$	Cross-sectional area
$[C]$	Overall damping matrix
$[C_e]$	Damping matrix of the element
$d_i$	Distance between the left end of the $i$ th element and the right end of the beam
$E$	Young's modulus
$I$	Area moment of inertia
$[I]$	Identity matrix
$(i, j, k)$	Unit vector along the $X, Y$ and $Z$ directions, respectively
$(i', j', k')$	Unit vector along the $x, y$ and $z$ directions, respectively
$K_E$	Kinetic energy
$K_{Ei}$	Kinetic energy of the $i$ th element
$[K]$	Overall stiffness matrix
$[K_e]$	Stiffness matrix of the element
$L$	Instantaneous length of the protruded part of the beam
$L_a$	Axial-oscillation amplitude of the beam with periodical motion
$L_B$	Total length of the beam
$L_i$	Distance between the left end of the $i$ th element and the rigid wall
$L_t$	Velocity of the beam
$l$	Length of the element
$l_i$	Length of the $i$ th element

$[M]$	Overall mass matrix	$(B_{e2}, \Gamma_{e2})$	Nodal rotational displacements at the right-hand ends of the element
$[M_e]$	Mass matrix of the element	$(\beta, \gamma)$	Rotational displacements with respect to the $(y, z)$ axes
$n$	Total number of elements	$(\beta_e, \gamma_e)$	Rotational displacements corresponding to the element coordinate system
$[N]$	Shape-function	$[\Phi]$	Floquet transition matrix
$P$	Axial load applied at the left end of the beam	$\lambda$	Eigenvalues
$\{q\}$	Overall displacement vector	$\rho$	Mass density
$\{q_e\}$	Nodal displacement vector	$\Omega$	Spin speed of the beam
$\mathbf{R}'$	Position vector of any material point of a beam after deformation	$\omega$	Natural frequency of free vibration
$\mathbf{r}'$	Position vector of any material point of a beam before deformation	$\omega_a$	Axial-oscillation frequency of the beam with periodical motion
$S_E$	Strain energy		
$S_{Ei}$	Strain energy of the $i$ th element		
$s$	Element coordinate		
$T$	Period		
$t$	Time		
$U$	Displacement field of a beam		
$U_a$	Potential energy due to the axial inertia force		
$U_{ai}$	Potential energy of the $i$ th element due to the axial inertia force		
$(V, W)$	Transverse displacements along the $(Y, Z)$ directions		
$(V_e, W_e)$	Transverse displacements corresponding to the element coordinate system		
$(V_{e1}, W_{e1})$	Nodal transverse displacements at the left-hand ends of the element		
$(V_{e2}, W_{e2})$	Nodal transverse displacements at the right-hand ends of the element		
$(v, w)$	Transverse displacements along the $(y, z)$ directions		
$(v_e, w_e)$	Transverse displacements corresponding to the element coordinate system		
$(X, Y, Z)$	Fixed coordinate system		
$(x, y, z)$	Rotating coordinate system		
$(B, \Gamma)$	Rotational displacements with respect to the $(Y, Z)$ axes		
$(B_e, \Gamma_e)$	Rotational displacements corresponding to the element coordinate system		
$(B_{e1}, \Gamma_{e1})$	Nodal rotational displacements at the left-hand ends of the element		

## 軸向移動與旋轉雷立夫樑 之振動與穩定性分析

張哲榮

中華民國空軍航空技術學院 飛機工程系

林暉智

中國鋼鐵股份有限公司 工程師

陳膺中

中華民國空軍軍官學校 航空機械工程學系

崔兆崇

國立成功大學 航空太空工程學系

黃俊榮

遠東科技大學 飛機修護系

### 摘要

本文採用雷立夫樑理論與可變域元素之有限元素法推導出具圓形截面的軸向移動和旋轉樑之運動方程式，其中考慮樑之旋轉慣性與陀螺效應，並藉由不同類型的軸向運動來觀察系統的動態行為。對具有定速軸向延伸的旋轉樑，求其運動方程式的特徵值來確認其穩定性，並用 Floquet 理論來分析具有週期性軸向移動旋轉樑的穩定性。本文探討了樑的旋轉速度對其振動與穩定性的影響，並使用直接時間數值積分方法 (Runge-Kutta) 來確認 Floquet 理論的結果。